

Miniature refractometer based on modal interference in a hollow-core photonic crystal fiber with collapsed splicing

Huaping Gong,^a Chi Chiu Chan,^b Yi Fan Zhang,^b Wei Chang Wong,^b and Xinyong Dong^a

^aChina Jiliang University, Institute of Optoelectronic Technology, Xueyuan Street, Xiasha Higher Education Zone, Hangzhou 310018, China

^bNanyang Technological University, School of Chemical and Biomedical Engineering, Division of Bioengineering, Singapore 637457, Singapore

Abstract. A miniature modal interferometer based on a hollow-core photonic crystal fiber (HC-PCF) for refractive index measurement is demonstrated. The modal interferometer is fabricated by splicing the two ends of a 1.2-mm-long HC-PCF to a single-mode fiber (SMF). The air holes of the HC-PCF are fully collapsed by the discharge arc during the splicing procedure, and the length of each collapsed region is about 300 μm . The transmission spectra with different refractive indices outside the HC-PCF are measured. Measurement resolutions of an 8.1×10^{-4} refractive index unit (RIU) in the range of 1.35 to 1.39, and 4.3×10^{-4} RIU in the range of 1.39 to 1.43 are achieved, respectively. The temperature effect of the proposed refractometer is also analyzed. © 2011 Society of Photo-Optical Instrumentation Engineers (SPIE). [DOI: 10.1117/1.3527259]

Keywords: photonic crystal fiber; modal interference; refractometer; collapsed splicing.

Paper 10282R received May 26, 2010; revised manuscript received Oct. 20, 2010; accepted for publication Nov. 15, 2010; published online Jan. 18, 2011.

1 Introduction

Optical fiber refractometers are widely employed in chemical and biological applications, owing to advantages such as easy fabrication, low cost, high sensitivity, safety in hazardous environments, and immunity to electromagnetic interference. Many fiber refractometers have been presented, for example, a fiber Bragg grating based refractometer,¹ a fiber Fabry-Perot structure,^{2,3} a refractometer based on long period grating,^{4,5} an abrupt taper Michelson interference-based refractometer,⁶ and a single-mode/multimode/single-mode fiber structure refractometer.^{7,8} Recently, a refractometer based on a large-mode-area photonic crystal fiber (PCF) (LMA-8) was also demonstrated, and the corresponding measurement resolution of the 32-mm-long interferometer was about 2.9×10^{-4} refractive index units (RIUs) in the refractive index range of 1.38 to 1.44.⁹ A reflective modal interferometer based on a 22-mm solid-core photonic crystal fiber (SC-PCF) was also proposed and used for refractive index measurement¹⁰ and volatile organic compound (VOC) detection.¹¹

Recently, hollow-core photonic crystal fiber (HC-PCF)-based modal interference has been investigated for potential in sensing applications. A modal interferometer based on a 27.8-cm-long HC-PCF has been presented,¹² employing strain and temperature measurements. The interference fringe still appeared, even when using a butt-coupling method instead of fusion splicing. The characteristic of HC-PCF was unique¹³ and different from SC-PCF-based modal interferometers, which were built by some special coupling methods.¹⁴

In this work, a miniature refractometer based on modal interference in the HC-PCF is demonstrated. A special splicing method is used to produce complete collapse of air holes in the core and cladding of the HC-PCF. Due to the complete collapse effect, this proposed interferometer is highly sensitive to the change of refractive index outside the fiber. The sensor fabrication and principle are described. Results and discussion are presented, and a conclusion is given.

2 Sensor Fabrication and Principle

The 1.2-mm HC-PCF-based modal interferometer was fabricated by splicing the two ends of a HC-PCF (HC-1550-02, Crystal Fiber A/S, NKT Photonics, Birkerød, Denmark) to a single-mode fiber (SMF). The core diameter of a HC-PCF is about 10.9 μm with a pitch of 3.8 μm , with a larger than 90% air filling fraction. The coating of the HC-PCF was stripped before splicing. The fiber end of the HC-PCF was cleaved by a CT-30 cleaver (Fujikura, Fairfield, Connecticut), and spliced to the SMF with a manual operation program described in Ref. 15. Then another fiber end of the HC-PCF was cleaved with fiber length control, and the total length of the HC-PCF was about 1.2 mm. The next procedure was the splicing for the second point under the same program. Fusion splicing was performed by using a Sumitomo Type-36 splicer (Sumitomo Electric Lightwave, Research Triangle Park, North Carolina), and the parameter settings for fusion splicing were the default parameters for the splicing of two standard SMFs. The insertion loss of the fabricated sensor was about 30 dB; it is very high because of air hole collapse and power leakage. The air holes of the HC-PCF were completely collapsed and the length of each collapsed region was about 300 μm , as shown in Fig. 1. Air hole collapse can be

Address all correspondence to: Chi Chiu Chan, Nanyang Technological University, School of Chemical and Biomedical Engineering, 50 Nanyang Drive, Research TechnoPlaza, Singapore, Singapore 639798. Tel: (65) 6790 4822; E-mail: eccchan@ntu.edu.sg.

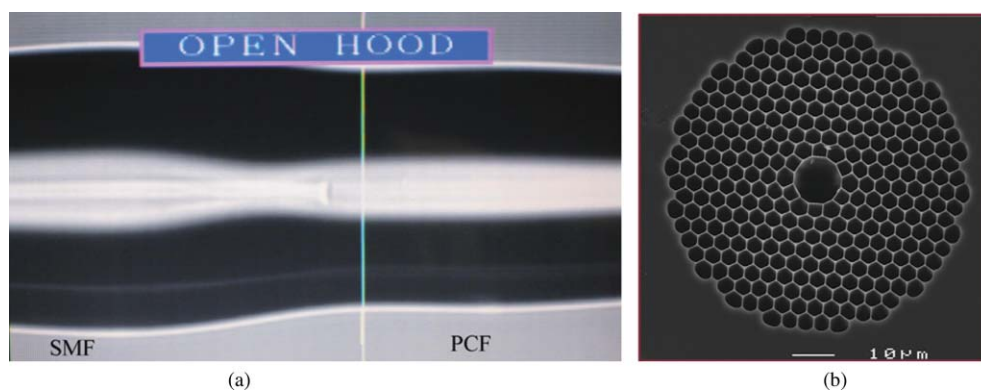


Fig. 1 (a) The image after splicing HC-PCF to SMF and (b) cross-section image of HC-PCF.

verified by using a microscope to observe the fiber end. After complete collapse, the HC-PCF becomes a stub of glass, and the outer diameter of the HC-PCF is less than that of the SMF.

Figure 2 shows the experimental setup and the structure of the 1.2-mm HC-PCF-based interferometer for refractive index measurement. The length of the sensing section was about 600 μm with the exception of the spliced area. The light from the broadband light source was passed through the SMF to the HC-PCF. The light transmitted from the HC-PCF entered into an optical spectrum analyzer (OSA, AQ6370, Yokogawa Company, Limited, Tokyo, Japan), and the corresponding transmission spectrum was acquired by the OSA. The broadband light source was an amplified spontaneous emission (ASE), which has a wavelength range of 1520 to 1600 nm.

When the light passed through the input SMF and entered into the collapsed region (part A in Fig. 2) of the HC-PCF, the fundamental core mode spread widely, and then the higher-order cladding modes were excited inside the HC-PCF. After the propagation of these modes inside the HC-PCF, they recombined at the second collapsed region (part B in Fig. 2) and propagated in the output SMF. Therefore, the modal interference was formed as described in Refs. 12 and 13. The transmission of the modal interferometer is expressed by the interference of two dominated modes,⁹

$$T = I_{co}(\lambda) + I_{cl}(\lambda) + 2[I_{co}(\lambda)I_{cl}(\lambda)]^{1/2} \cos(2\pi \Delta n_{\text{eff}}L/\lambda), \quad (1)$$

and the maxima of transmission will appear at wavelengths $\lambda_m \approx \Delta n_{\text{eff}}L/m$, where m is an integer. Therefore, the fringe

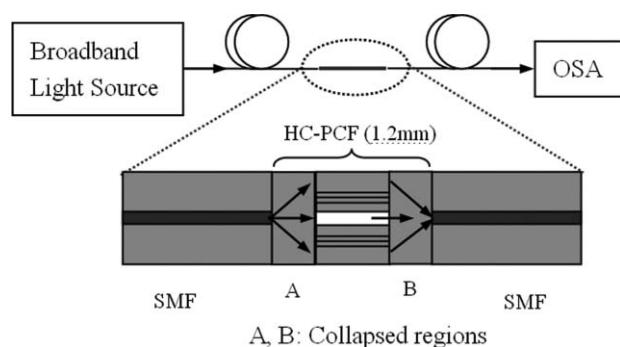


Fig. 2 Experimental setup and configuration of the 1.2-mm HC-PCF-based modal interferometer.

periodicity (S) of the modal interference is associated with the refractive index difference between these modes, which can be described as,¹⁰

$$S \approx \lambda^2/(\Delta n_{\text{eff}}L), \quad (2)$$

where Δn_{eff} is the effective index difference between these modes, and λ is the operating wavelength. It can be seen that the modal interferometer is sensitive to the variations of Δn_{eff} and L . Due to the complete collapse of the air holes of the HC-PCF, the fundamental core mode is spread out and the cladding modes of HC-PCF are exited efficiently. Also, the evanescent waves of the cladding modes reach the external surface of the HC-PCF, which can interact with liquid specimens outside the HC-PCF. When the refractive index liquid is deposited on the outer surface of the HC-PCF, Δn_{eff} can be varied. Then the peaks in the transmission spectrum are shifted. Therefore, the refractive index measurement can be realized by measuring the corresponding wavelength shift.

3 Results and Discussion

The refractive index liquid samples (Cargille Laboratories, Cedar Grove, New Jersey), which have refractive indices of 1.35, 1.37, 1.39, 1.41, and 1.43, were used for the refractive index

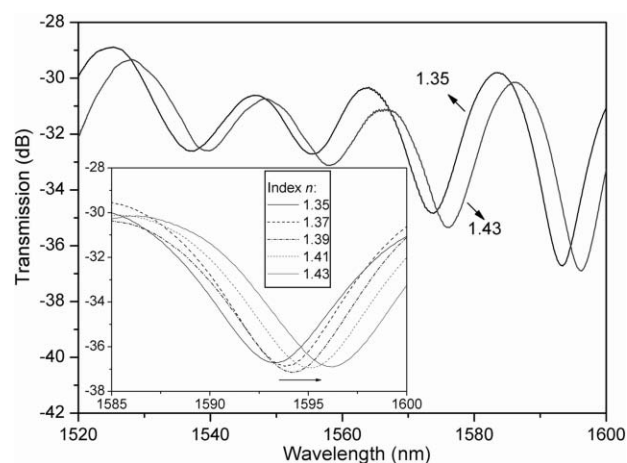


Fig. 3 Transmission spectra of the HC-PCF-based interferometer with different refractive indices; inset is a close-up display of the dip near 1595 nm.

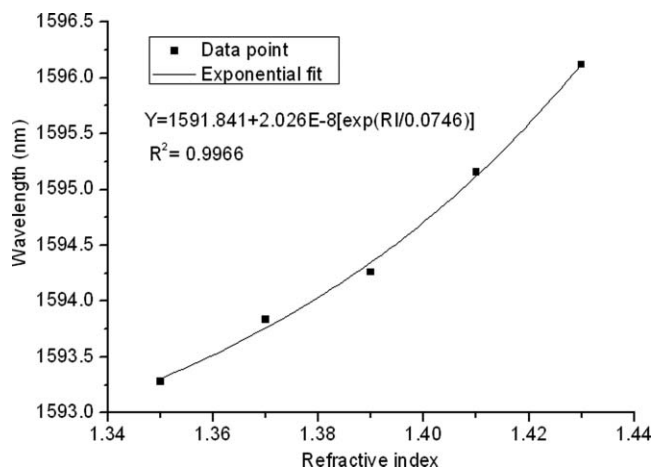


Fig. 4 Wavelength shift of the HC-PCF-based interferometer versus refractive index.

measurement of the HC-PCF-based refractometer. The calibrated refractive index accuracy for each liquid was ± 0.0002 refractive index units (RIUs). Figure 3 shows the transmission spectra of a HC-PCF-based interferometer with different refractive indices outside the HC-PCF at room temperature. It appears that the interference fringes with good visibility and the maximum extinction ratio is about 7 dB. The wavelength separation between the adjacent peaks or dips is about 20 nm. When the refractive index was varied from 1.35 to 1.43, the dip wavelength shifted from 1593.28 to 1596.16 nm, corresponding a total red shift of 2.88 nm, as shown in Fig. 4. The red shift is observed because the increase of the refractive index leads to the increase of Δn_{eff} . The wavelength shift of the interference fringe becomes larger with the increase of the refractive index, so the sensitivity for the range of 1.35 to 1.39 is higher than that for the range of 1.35 to 1.39, which is similar to the SC-PCF-based refractometer.⁹ The sensitivities of 24.5 and 46.5 nm/RIU for the index range of 1.35 to 1.39 and 1.39 to 1.43 are achieved, respectively. Thus, the resolutions of refractive index measurement for the range of 1.35 to 1.39 and 1.39 to 1.43 are about 8.1×10^{-4} and 4.3×10^{-4}

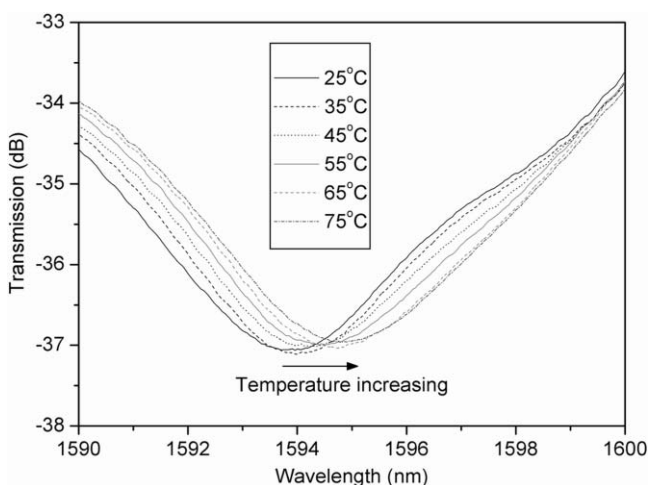


Fig. 5 Transmission spectra of the HC-PCF-based interferometer with different temperatures.

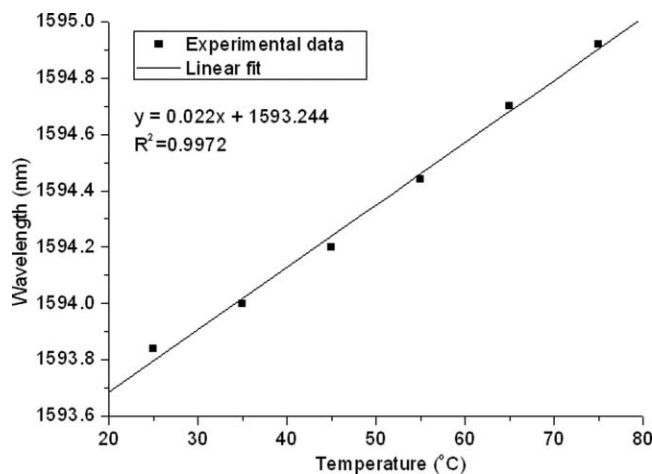


Fig. 6 Wavelength shift versus temperature.

RIUs, respectively, considering a wavelength resolution of 20 pm of the OSA used in the experiment, which is comparable to other refractometers.^{1,2,4-6,9-11} In addition, the lengths of the sensing fibers of the other refractometers, such as single-mode/multimode/single-mode-based refractometers^{7,8} and SC-PCF modal interference-based refractometers,⁹⁻¹¹ are approximately dozens of millimeters, while that of the HC-PCF modal interference-based refractometer is just about 600 μm . The small-sized refractometer has an advantage in chemical and biological applications, because it needs only one microliter samples.

Figure 5 shows the wavelength shift of the dip with the increase of external temperature. The peaks or dips in the transmission spectrum are shifted because the effective indices of these modes are dependent on the temperature effect, and the thermal expansion leads to variation of fiber length. When the temperature was increased from 25 to 75°C, the wavelength of the dip in the transmission was changed from 1593.84 to 1594.92 nm, corresponding to a red shift of about 1.08 nm. The wavelength shift of the dip has a linear relationship with the temperature change, and a sensitivity of about 22 pm/°C is achieved, as shown in Fig. 6. The temperature variation can affect the resolution of the refractive index measurement. The corresponding refractive index measurement error due to the temperature effect is about 8.9×10^{-4} RIU/°C. However, our experiments were conducted in a temperature-controlled environment; the corresponding temperature variation was about 0.2°C, so the refractive index measurement error by the effect of temperature was about 1.8×10^{-4} RIU, which is less than that limited by the wavelength resolution of the OSA. Therefore, our experimental results of refractive index measurement are reliable, and the temperature effect can be ignored if the temperature variation is less than 1°C.

4 Conclusions

A 1.2-mm HC-PCF-based miniature modal interferometer for refractive index measurement is demonstrated. The complete collapse of air holes in the HC-PCF introduces a high sensitivity to refractive index change outside the HC-PCF. The resolutions of refractive index measurement for the ranges of 1.35 to 1.39 and 1.39 to 1.43 are about 8.1×10^{-4} RIU and 4.3×10^{-4} RIUs,

respectively. The index measurement error due to the temperature effect is about 8.9×10^{-4} RIU/°C. Therefore, the temperature effect could be ignored if the temperature variation is less than 1°C. Moreover, the proposed miniature refractometer has advantages such as reuse, small size, robustness, easy fabrication, and an all-fiber and all-sealed structure, so it is very suitable for chemical and biological applications.

Acknowledgment

This work was supported by the Network Technology Research Center, School of Electrical and Electronic Engineering, Nanyang Technological University, and also supported by the China 973 program (grant number 2010CB327804).

References

1. W. Liang, Y. Huang, Y. Xu, R.K. Lee, and A. Yariv, "Highly sensitive fiber Bragg grating refractive index sensors," *Appl. Phys. Lett.* **86**(15), 151122 (2005).
2. O. Frazão, P. Caldas, J. L. Santos, P. V. S. Marques, C. Turck, D. J. Lougnot, and O. Soppera, "Fabry-Perot refractometer based on an end-of-fiber polymer tip," *Opt. Lett.* **34**(16), 2474–2476 (2009).
3. M. Deng, C. P. Tang, T. Zhu, Y. J. Rao, L. C. Xu, and M. Han, "Refractive index measurement using photonic crystal fiber-based Fabry-Perot interferometer," *Appl. Opt.* **49**(9), 1593–1598 (2010).
4. L. Mosquera, D. Sáez-Rodríguez, J. L. Cruz, and M. V. Andrés, "In-fiber Fabry-Perot refractometer assisted by a long-period grating," *Opt. Lett.* **35**(4), 613–615 (2010).
5. J. F. Ding, A. P. Zhang, L. Y. Shao, J. H. Yan, and S. He, "Fiber-taper seeded long-period grating pair as a highly sensitive refractive-index sensor," *IEEE Photon. Technol. Lett.* **17**(6), 1247–1249 (2005).
6. Z. Tian, S. S. H. Yam, and H-P. Loock, "Refractive index sensor based on an abrupt taper Michelson interferometer in a single-mode fiber," *Opt. Lett.* **33**(10), 1105–1107 (2008).
7. Q. Wang and G. Farrell, "All-fiber multimode-interference based refractometer sensor: proposal and design," *Opt. Lett.* **31**(3), 317–319 (2006).
8. J. Villatoro and D. Monzón-Hernández, "Low-cost optical fiber refractive-index sensor based on core diameter mismatch," *J. Light-wave Technol.* **24**(3), 1409–1413 (2006).
9. R. Jha, J. Villatoro, G. Badenes, and V. Pruneri, "Refractometry based on a photonic crystal fiber interferometer," *Opt. Lett.* **34**(5), 617–619 (2009).
10. R. Jha, J. Villatoro, and G. Badenes, "Ultrastable in reflection photonic crystal fiber modal interferometer for accurate refractive index sensing," *Appl. Phys. Lett.* **93**(19), 191106 (2008).
11. J. Villatoro, M. P. Kreuzer, and R. Jha, "Photonic crystal fiber interferometer for chemical vapor detection with high sensitivity," *Opt. Express* **17**(3), 1447–1453 (2009).
12. S. H. Aref, R. Amezcua-Correa, J. P. Carvalho, O. Frazão, P. Caldas, J. L. Santos, F. M. Araújo, H. Latifi, F. Farahi, L. A. Ferreira, and J. C. Knight, "Modal interferometer based on hollow-core photonic crystal fiber for strain and temperature measurement," *Opt. Express* **19**(21), 18669–18675 (2009).
13. R. Amezcua-Correa, F. Gèrôme, S. G. Leon-Saval, N. G. R. Broderick, T. A. Birks, and J. C. Knight, "Control of surface modes in low loss hollow-core photonic bandgap fibers," *Opt. Express* **16**(2), 1142–1149 (2008).
14. J. Villatoro, V. Finazzi, G. Badenes, and V. Pruneri, "Highly sensitive sensors based on photonic crystal fiber modal interferometers," *J. Sensors* **2009**, 747803 (2009).
15. Y. Wang, H. Bartelt, S. Brueckner, J. Kobelke, M. Rothhardt, K. Mörl, W. Ecke, and R. Willsch, "Splicing Ge-doped photonic crystal fibers using commercial fusion splicer with default discharge parameters," *Opt. Express* **16**(10), 7258–7263 (2008).